



Crystal structure and Hirshfeld surface analysis of (*S*)-*N*-methyl-1-phenylethan-1-aminium chloride

Jan-Lukas Kirchhoff, Lukas Brieger and Carsten Strohmann*

Technische Universität Dortmund, Fakultät Chemie und Chemische Biologie, Otto-Hahn-Strasse 6, 44227 Dortmund, Germany. *Correspondence e-mail: carsten.strohmann@tu-dortmund.de

Received 29 November 2021

Accepted 28 December 2021

Edited by D. Chopra, Indian Institute of Science Education and Research Bhopal, India

Keywords: crystal structure; chiral amines; Hirshfeld atom refinement (HAR); *NoSpherA2*; separation strategies; Hirshfeld surface analysis.

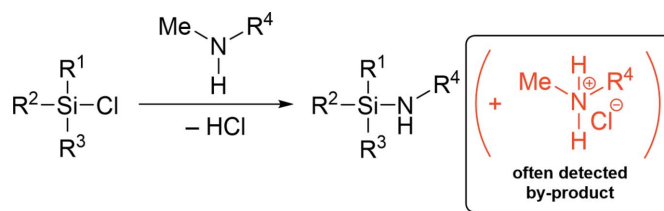
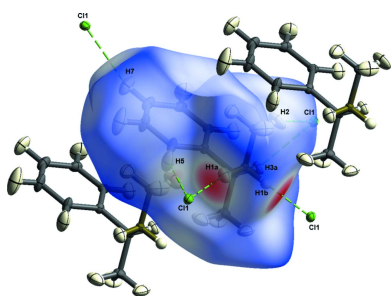
CCDC reference: 2132333

Supporting information: this article has supporting information at journals.iucr.org/e

The title compound $C_9H_{14}N^+ \cdot Cl^-$, (**1**), can be synthesized starting from (*S*)-*N*-methyl-1-phenylethan-1-amine (**2**). Compound **2** upon addition of $HCl \cdot Et_2O$ leads to crystallization of compound **1** as colorless blocks. The configuration of compound **1** is stable as well as preserved in space group $P2_12_12_1$. Ammonium chlorides, like the title compound, are often observed as undesirable by-products in aminosilylation of chlorosilanes. Additionally, these by-products are usually soluble in selected organic solvents, which require difficult separation steps. Therefore, detailed studies on structural features and intermolecular interactions performed by Hirshfeld atom refinement (HAR) using *NoSpherA2* [Kleemiss *et al.* (2021). *Chem. Sci.* **12**, 1675–1692] and Hirshfeld surface analysis were used to address structural issues on that separation problem.

1. Chemical context

Chiral amines represent a central role in synthetic chemistry, finding more and more applications in asymmetric syntheses (Liu *et al.*, 2020). In addition to asymmetric inductions on double bonds of organic molecules, they also serve as amination reagents of chlorosilanes (Wannagat & Klemke, 1979; Veith, 1987). Next to methoxysilanes, those chlorosilanes are the most important starting compounds for the synthesis of aminosilanes (Bauer & Strohmann, 2012). The title compound (*S*)-*N*-methyl-1-phenylethan-1-aminium chloride (**1**), represents the ammonium chloride salt of (*S*)-*N*-methyl-1-phenylethan-1-amine (**2**), which is often used as a chiral auxiliary in reagent inductions on prochiral silicon centers (Bauer & Strohmann, 2014). Compound **2** and its derivatives are characterized by well-known methods of enantiomeric resolution (Ingersoll, 1937; Baltzly & Russell, 1953). The synthesis of Si–N-functionalized silanes starting from chlorosilanes in combination with amines is also very well known (Sakaba *et al.*, 2015; Zibula *et al.*, 2020). However, the formation of the undesirable ammonium chloride is often observed as a by-product, which is also soluble in small amounts of selected organic solvents. The corresponding reaction is shown in the scheme below.



Compound **1** was crystallized for the first time and may be used to analyze supramolecular interactions, in particular those which could be directly related to the aforementioned separation problem. To describe the positions of the hydrogen atoms as accurately as possible, all hydrogen atoms were refined anisotropically by *NoSpherA2* (Kleemiss *et al.*, 2021).

2. Structural commentary

Compound **1** crystallized from diethyl ether at room temperature in the shape of colorless blocks with orthorhombic ($P2_12_12_1$) symmetry. The absolute configuration of the chiral ammonium chloride **1** in the measured crystal can be assigned with the (*S*)-configuration using the Cahn–Ingold–Prelog (CIP) prioritization (Cahn *et al.*, 1966); the Flack parameter amounts to -0.03 (3) (Flack, 1983). The molecular structure of **1** is illustrated in Fig. 1. All hydrogen atoms except H1*b* were refined using *NoSpherA2* (Kleemiss *et al.*, 2021). No particularly large ellipsoids are observed here, whereas hydrogen atom H1*b* is highly deformed and distorted in anisotropic treatment. The substantial contribution from deformation of the electron density involving the chloride ion, which also includes polarization, may be responsible for the

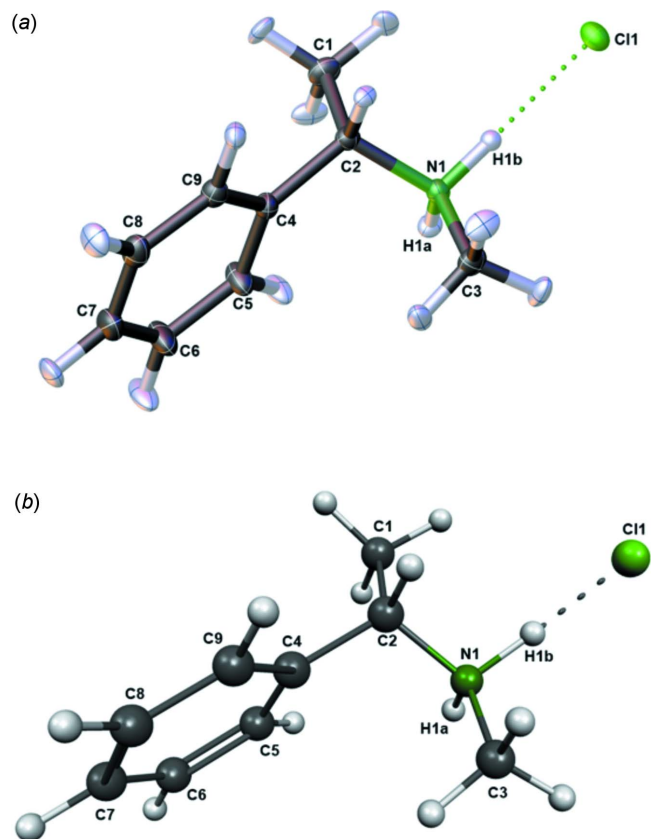


Figure 1
(a) The molecular structure of **1** illustrated showing 50% displacement ellipsoids including. All hydrogen atoms except H1*b* were refined by Hirshfeld atom refinement (HAR) performed by *NoSpherA2* implementation in *OLEX2*. (b) Visualization of the calculated structure of compound **1** with *Molekel 4.3* performed at the M062X/6–31+G(*d*) levels.

Table 1
Hydrogen-bond geometry (Å, °).

$D-H\cdots A$	$D-H$	$H\cdots A$	$D\cdots A$	$D-H\cdots A$
$N1-H1a\cdots Cl1^i$	1.029 (6)	2.088 (6)	3.1075 (3)	170.4 (5)
$N1-H1b\cdots Cl1$	1.031 (6)	2.062 (6)	3.0925 (4)	177.8 (5)

Symmetry code: (i) $-x + 1, y - \frac{1}{2}, -z + \frac{1}{2}$.

observed ellipsoidal shape of the hydrogen atom H1*b*. Thus it is difficult to deconvolute the effect of thermal motion in this interaction and to model the same satisfactorily. Therefore, the hydrogen atom H1*b* was isotropically modeled for following analyses as shown in Fig. 1(a).

In the literature, known Csp^3-N bond lengths are in a range of 1.4816 (4) Å (N1–C3) and 1.5034 (4) Å (N1–C2), which are typical for most structurally analyzed ammonium salts (Allen *et al.*, 1987). To discuss the bond distances in the solid-state structure, quantum chemical calculations were performed at the level M062X/6–31+G(*d*), which gave comparable results. The molecular structure of compound **1** in the gas phase is shown in Fig. 1(b). All conformations were taken from the solid-state structure at the start of the optimization. The result of the calculation provides smaller Csp^3-N bond lengths than from the solid-state structure in principle. The calculated bond lengths are 1.4762 Å (N1–C3) and 1.4946 Å (N1–C2).

Hydrogen-bond lengths as well as associated angles are shown in Table 1. The calculated hydrogen bond of 1.7051 Å (N1–H1*b*···Cl1) was not described sufficiently with the addition of the used potential and basis set. Therefore, a large deviation can be observed from the analyzed distance compared to the crystal structure. Further analyses concerning supramolecular interactions are discussed in detail in the next section.

The stereogenic carbon center features a tetrahedral geometry, which is slightly distorted as shown by the angle of 107.44 (2)° (C1–C2–N1). However, the geometric distortion of a tetrahedral carbon center has been observed in many compounds with different substituents (Xu *et al.*, 2000).

3. Supramolecular features

The crystal packing along the *a*-axis of compound **1** is shown in Fig. 2. To analyze supramolecular packing interactions in more detail, Hirshfeld surface analyses were performed. The Hirshfeld surface mapped over d_{norm} in the range from -0.5483 to 1.5337 arbitrary units generated by *CrystalExplorer2021* (Spackman *et al.*, 2021; Turner *et al.*, 2017) is shown in Fig. 3. Fingerprint plots, which are illustrated in Fig. 4, were also generated by *CrystalExplorer2021*. First, the crystal structure was analyzed to clarify for the influence of hydrogen bonds. Particularly noticeable on the Hirshfeld surface are C–H···Cl contacts, which are shown in red on the potential surface in Fig. 3.

The primary share of 66.9% can be assigned to weak van der Waals H···H contacts, which should play a minor role in

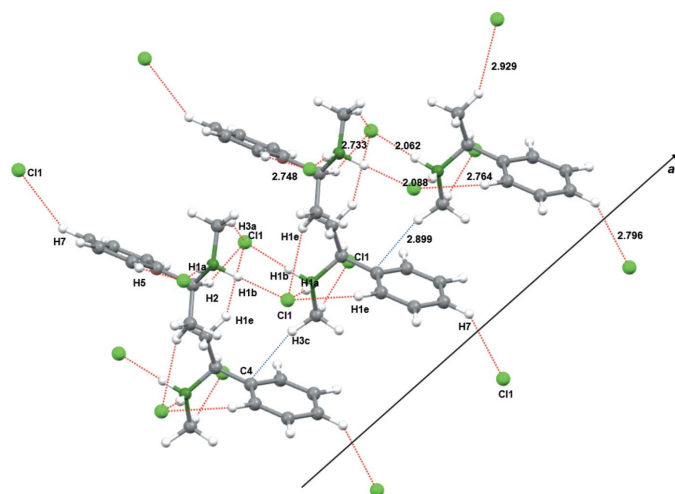


Figure 2
A view along the *a*-axis direction of the crystal packing of compound **1**. Selected hydrogen-bond lengths (in Å) are indicated.

terms of crystal packing. In contrast, Cl \cdots H/H \cdots Cl contacts in particular, which represent the smallest fraction of interactions (15.1%), however represent the most intense contacts on the surface (Fig. 4). Hydrogen bonds with a length up to 2.200 Å are shown in Table 1. The analysis of the hydrogen-bonding network leads to the result that all hydrogen bridges can be assigned to one graph-set motif. Both hydrogen bonds in Table 1 can be assigned $D_1^1(2)$ (Etter *et al.*, 1990).

In addition to the influence of C–H \cdots Cl contacts, the influence of possible π -interactions was analyzed by *CrystalExplorer2021*. As can be seen in Fig. 2, compound **1** forms one-dimensional chains along the *a*-axis direction in the crystal structure. These can be attributed to the strong C–H \cdots Cl interactions already mentioned, as well as additional C–H \cdots π interactions, which are illustrated in Fig. 2. Consequently, these π -interactions could contribute a significant

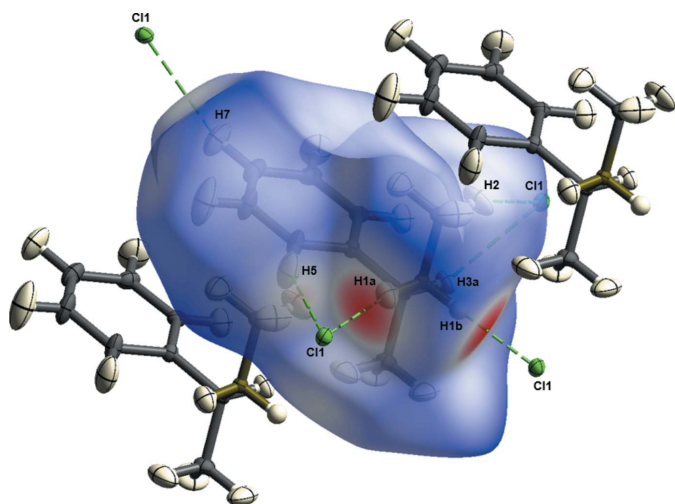


Figure 3
Hirshfeld surface of compound **1** generated by *CrystalExplorer21*.

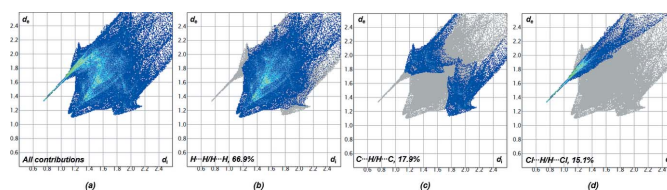


Figure 4
Two-dimensional fingerprint plots of compound **1** showing close contacts of (a) all contributions in the crystal and those delineated into (b) H \cdots H, (c) C \cdots H/H \cdots C and (d) Cl \cdots H/H \cdots Cl-interactions. Symmetry codes: (i) $\frac{1}{2} - x, -y, \frac{1}{2} + z$; (ii) $-x, \frac{1}{2} + y, \frac{1}{2} - z$; (iii) $\frac{1}{2} + x, \frac{1}{2} - y, -z$.

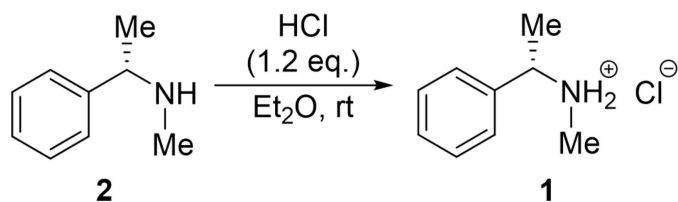
part to the crystal packing structure. However, C–H \cdots π contacts are only weakly visible on the Hirshfeld surface.

4. Database survey

There are some crystallographically characterized examples based on the structure of compound **1**. Depicted examples found in Cambridge Structural Database (WebCSD, November 2021; Groom *et al.*, 2016) include *N,N'*-bis(1-phenylethyl)cyclohex-4-ene-1,2-diaminium dichloride monohydrate, C₂₂H₃₂N₂O₂Cl (CSD refcode KIZHIM; Savoia *et al.*, 2014), 2-(ethoxycarbonyl)-*N*-(1-phenylethyl)cyclopentan-1-aminium chloride, C₁₆H₂₄ClNO₂ (BAJSIS; Lee *et al.*, 2021), *N*-[(*R*)-(cyclohexan-*R*)-2-ol]-(*R*)- α -methylbenzyl ammonium chloride, C₁₄H₂₂NOCl (TAYWOF; Barbaro *et al.*, 1996), [2-(1*H*-inden-3-yl)ethyl][(1*R*)-1-phenylethyl]ammonium chloride, C₁₉H₂₂NCl (GOGCUC; Ross *et al.*, 2015), *cis*-(*aR*,1*R*,2*S*)-2-methoxy-1-(1-phenylethylamino)cyclopentane-carboxamide hydrochloride, C₁₅H₂₃N₂O₂Cl (NAFZIE; Meyer *et al.*, 2004). A comparison with the last two structures mentioned shows that compound **1** is characterized by particularly short C–H \cdots Cl (2.0–2.1 Å) hydrogen bonds. The smallest observed hydrogen bond of the two literature known compounds amounts to 2.2 Å. These longer distances could be due to the more sterically demanding substituents, which are less pronounced in compound **1**. Moreover, in terms of the crystal packing, the compounds do not exhibit one-dimensional chains, as C–H \cdots π contacts were not observed. This unique feature of (*S*)-*N*-methyl-1-phenylethan-1-aminium chloride (**1**), which does not appear in the literature compounds, could again be attributed to the steric crowding of the other compounds.

5. Synthesis and crystallization

The reaction scheme for the synthesis of compound **1** is illustrated in the scheme below. (*S*)-*N*-methyl-1-phenylethan-1-amine (**2**) (1.48 mmol) was dissolved in diethyl ether (5 mL). A 2 *M* solution of HCl in diethyl ether (1.78 mmol) was added dropwise. The solution was stored at 298 K for three days. Afterwards all volatile compounds were removed and the raw product was washed with cold *n*-pentane (1 ml). (*S*)-*N*-methyl-1-phenylethan-1-aminium chloride (**1**) was isolated as colorless crystalline plates.



^1H NMR (300.13 MHz, CDCl_3): δ = 1.88 (s, 3H, CHCH_3), 2.46 (s, 3H, NCH_3), 1.65–1.90 (br. s, 1H, CHCH_3), 7.38–7.45 (m, 3H, CH_{ar} , meta, CH_{ar} , para), 7.60 (d, 2H, $^3J_{\text{H-H}}$ = 3.9 Hz, CH_{ar} , ortho), 9.78 (br. s, 1H, $\text{NH}\cdots\text{Cl}$), 10.17 (br. s, 1H, $\text{NH}\cdots\text{Cl}$) ppm.

$\{1\text{H}\}^{13}\text{C}$ NMR (100.64 MHz, CDCl_3): δ = 20.5 (1C, CHCH_3), 31.0 (1C, CHCH_3), 60.2 (2C, NCH_3), 127.9 (2C, $\text{C}_{\text{ortho}}\text{H}_{\text{ar}}$), 129.5 (2C, $\text{C}_{\text{meta}}\text{H}_{\text{ar}}$), 135.6 (1C, $\text{C}_{\text{para}}\text{H}_{\text{ar}}$) ppm.

CHN analysis: calculated: C = 62.97%, H = 8.22% N = 8.16%; Found: C = 62.6%, H = 7.9%, N = 7.8%.

R_f : (CH_2Cl_2 / MeOH; 10:1) = 0.20.

6. Refinement

Crystal data, data collection and structure refinement details are summarized in Table 2. All H atoms except H1b were refined freely using independent values of each $U_{\text{iso}}(\text{H})$. Hirshfeld atom refinements (HAR; Fugel *et al.*, 2018) was performed with the *NoSpherA2* (Kleemiss *et al.*, 2021) implementation in *OLEX2* (Dolomanov *et al.*, 2009), using the restricted Khom–Sham method with the PBE-functional (Perdew *et al.*, 1996) and basis set def2-SVP (Weigend & Ahlrichs, 2005). For the HAR approach, all H atoms except H1b were refined anisotropically and independently. Atom H1b was refined freely without using HAR by *NoSpherA2*.

Acknowledgements

J-LK, LB and CS thank the Fonds der Chemischen Industrie for two doctoral fellowships.

References

- Allen, F. H., Kennard, O., Watson, D. G., Brammer, L., Orpen, A. G. & Taylor, R. (1987). *J. Chem. Soc. Perkin Trans. 2*, pp. S1–19.
- Baltzly, R. & Russell, P. B. (1953). *J. Am. Chem. Soc.* **75**, 5598–5602.
- Barbaro, P., Bianchini, C. & Sernau, V. (1996). *Tetrahedron Asymmetry*, **7**, 843–850.
- Bauer, J. O. & Strohmman, C. (2012). *Chem. Commun.* **48**, 7212–7214.
- Bauer, J. O. & Strohmman, C. (2014). *Angew. Chem. Int. Ed.* **53**, 8167–8171.
- Bruker (2021). *APEX4*, *SAINT* and *SADABS*. Bruker AXS Inc., Madison, Wisconsin, USA.
- Cahn, R. S., Ingold, C. & Prelog, V. (1966). *Angew. Chem. Int. Ed. Engl.* **5**, 385–415.
- Dolomanov, O. V., Bourhis, L. J., Gildea, R. J., Howard, J. A. K. & Puschmann, H. (2009). *J. Appl. Cryst.* **42**, 339–341.
- Etter, M. C., MacDonald, J. C. & Bernstein, J. (1990). *Acta Cryst.* **B46**, 256–262.
- Flack, H. D. (1983). *Acta Cryst.* **A39**, 876–881.
- Flükiger, P., Lüthi, H. P., Portmann, S. & Weber, J. (2000). *MOLEKEL 4.3*. Swiss Center for Scientific Computing, Manno, Switzerland.

Table 2

Experimental details.

Crystal data	
Chemical formula	$\text{C}_9\text{H}_{14}\text{N}^+\cdot\text{Cl}^-$
M_r	171.67
Crystal system, space group	Orthorhombic, $P2_12_12_1$
Temperature (K)	100
a, b, c (Å)	6.7723 (6), 7.1806 (5), 20.542 (2)
V (Å ³)	998.96 (16)
Z	4
Radiation type	Mo $K\alpha$
μ (mm ⁻¹)	0.32
Crystal size (mm)	0.48 × 0.39 × 0.37
Data collection	
Diffractionmeter	Bruker D8 Venture
Absorption correction	Multi-scan (<i>SADABS</i> ; Bruker, 2021)
$T_{\text{min}}, T_{\text{max}}$	0.602, 0.650
No. of measured, independent and observed [$I \geq 2\sigma(I)$] reflections	45327, 4856, 4785
R_{int}	0.026
$(\sin \theta/\lambda)_{\text{max}}$ (Å ⁻¹)	0.834
Refinement	
$R[F^2 > 2\sigma(F^2)], wR(F^2), S$	0.011, 0.024, 1.14
No. of reflections	4856
No. of parameters	221
H-atom treatment	H atoms treated by a mixture of independent and constrained refinement
$\Delta\rho_{\text{max}}, \Delta\rho_{\text{min}}$ (e Å ⁻³)	0.14, -0.22
Absolute structure	Hoof et al., 2010
Absolute structure parameter	-0.011 (7)

Computer programs: *APEX4* and *SAINT* (Bruker, 2021), *SHELXS* (Sheldrick, 2008), *SHELXL* (Sheldrick, 2015), *OLEX2* (Dolomanov *et al.*, 2009), *CrystalExplorer21* (Spackman *et al.*, 2021; Turner *et al.*, 2017), *publCIF* (Westrip, 2010), *Mercury* (Macrae *et al.*, 2020), *NoSpherA2* (Kleemiss *et al.*, 2021), *GaussView 6.016* (Frisch *et al.*, 2016), *Gaussian 09* (Frisch *et al.*, 2016), *Molekel 4.3* (Flükiger *et al.*, 2000) and *PLATON* (Spek, 2020).

- Frisch, M. J., Trucks, G. W., Schlegel, H. B., Scuseria, G. E., Robb, M. A., Cheeseman, J. R., Scalmani, G., Barone, V., Petersson, G. A., Nakatsuji, H., Li, X., Caricato, M., Marenich, A., Bloino, J., Janesko, B. G., Gomperts, R., Mennucci, B., Hratchian, H. P., Ortiz, J. V., Izmaylov, A. F., Sonnenberg, J. L., Williams-Young, D., Ding, F., Lipparini, F., Egidi, F., Goings, J., Peng, B., Petrone, A., Henderson, T., Ranasinghe, D., Zakrzewski, V. G., Gao, J., Rega, N., Zheng, G., Liang, W., Hada, M., Ehara, M., Toyota, K., Fukuda, R., Hasegawa, J., Ishida, M., Nakajima, T., Honda, Y., Kitao, O., Nakai, H., Vreven, T., Throssell, K., Montgomery, J. A. Jr, Peralta, J. E., Ogliaro, F., Bearpark, M., Heyd, J. J., Brothers, E., Kudin, K. N., Staroverov, V. N., Keith, T., Kobayashi, R., Normand, J., Raghavachari, K., Rendell, A., Burant, J. C., Iyengar, S. S., Tomasi, J., Cossi, M., Millam, J. M., Klene, M., Adamo, C., Cammi, R., Ochterski, J. W., Martin, R. L., Morokuma, K., Far kas, O., Foresman, J. B. & Fox, D. J. (2016). *Gaussian 09*. Revision A.02. Gaussian, Inc., Wallingford, CT, USA.
- Fugel, M., Jayatilaka, D., Hupf, E., Overgaard, J., Hathwar, V. R., Macchi, P., Turner, M. J., Howard, J. A. K., Dolomanov, O. V., Puschmann, H., Iversen, B. B., Bürgi, H.-B. & Grabowsky, S. (2018). *IUCrJ*, **5**, 32–44.
- Groom, C. R., Bruno, I. J., Lightfoot, M. P. & Ward, S. C. (2016). *Acta Cryst.* **B72**, 171–179.
- Hoof, R. W. W., Straver, L. H. & Spek, A. L. (2010). *J. Appl. Cryst.* **43**, 665–668.
- Ingersoll, W. A. (1937). *Org. Synth.* **17**, 80.
- Kleemiss, F., Dolomanov, O. V., Bodensteiner, M., Peyrerimhoff, N., Midgley, L., Bourhis, L. J., Genoni, A., Malaspina, L. A., Jayatilaka,

- D., Spencer, J. L., White, F., Grundkötter-Stock, B., Steinhauer, S., Lentz, D., Puschmann, H. & Grabowsky, S. (2021). *Chem. Sci.* **12**, 1675–1692.
- Lee, H.-S., Kim, J. & Lim, D. (2021). *CSD Communication* (refcode: BAJISIS). CCDC, Cambridge, England.
- Liu, Y., Yue, X., Li, L., Li, Z., Zhang, L., Pu, M., Yang, Z., Wang, C., Xiao, J. & Lei, M. (2020). *Inorg. Chem.* **59**, 8404–8411.
- Macrae, C. F., Sovago, I., Cottrell, S. J., Galek, P. T. A., McCabe, P., Pidcock, E., Platings, M., Shields, G. P., Stevens, J. S., Towler, M. & Wood, P. A. (2020). *J. Appl. Cryst.* **53**, 226–235.
- Meyer, U., Breitling, E., Biesel, P. & Frahm, A. W. (2004). *Tetrahedron Asymmetry*, **15**, 2029–2037.
- Perdew, J. P., Burke, K. & Ernzerhof, M. (1996). *Phys. Rev. Lett.* **77**, 3865–3868.
- Ross, J. H., Rohjans, S. H., Schmidtman, M. & Doye, S. (2015). *Arkivoc*, **2015**, 76–92.
- Sakaba, H., Tonosaki, H., Isozaki, K. & Kwon, E. (2015). *Organometallics*, **34**, 1029–1037.
- Savoia, D., Balestri, D., Grilli, S. & Monari, M. (2014). *Eur. J. Org. Chem.* **2014**, 1907–1914.
- Sheldrick, G. M. (2008). *Acta Cryst.* **A64**, 112–122.
- Sheldrick, G. M. (2015). *Acta Cryst.* **C71**, 3–8.
- Spackman, P. R., Turner, M. J., McKinnon, J. J., Wolff, S. K., Grimwood, D. J., Jayatilaka, D. & Spackman, M. A. (2021). *J. Appl. Cryst.* **54**, 1006–1011.
- Spek, A. L. (2020). *Acta Cryst.* **E76**, 1–11.
- Turner, M. J., McKinnon, J. J., Wolff, S. K., Grimwood, D. J., Spackmann, P. R., Jayatilaka, D. & Spackman, M. A. (2017). *CrystalExplorer17*, University of Western Australia.
- Veith, M. (1987). *Angew. Chem. Int. Ed. Engl.* **26**, 1–14.
- Wannagat, U. & Klemke, S. (1979). *Monatsh. Chem.* **110**, 2868–2881.
- Weigend, F. & Ahlrichs, R. (2005). *Phys. Chem. Chem. Phys.* **7**, 3297–3305.
- Westrip, S. P. (2010). *J. Appl. Cryst.* **43**, 920–925.
- Xu, Z., Zhao, C. & Lin, Z. (2000). *J. Chem. Soc. Perkin Trans. 2*, pp. 2319–2323.
- Zibula, L., Achternbosch, M., Wattenberg, J., Otte, F. & Strohmann, C. (2020). *Z. Anorg. Allg. Chem.* **646**, 978–984.

supporting information

Acta Cryst. (2022). E78, 130-134 [https://doi.org/10.1107/S2056989021013645]

Crystal structure and Hirshfeld surface analysis of (S)-N-methyl-1-phenylethan-1-aminium chloride

Jan-Lukas Kirchoff, Lukas Brieger and Carsten Strohmann

Computing details

Cell refinement: *SAINTE* (Bruker, 2021); data reduction: *APEX4* (Bruker, 2021); program(s) used to solve structure: *SHELXS* (Sheldrick, 2008); program(s) used to refine structure: *SHELXL* (Sheldrick, 2015); molecular graphics: *OLEX2* (Dolomanov *et al.*, 2009); software used to prepare material for publication: *APEX4* (Bruker, 2021), *CrystalExplorer21* (Spackman *et al.*, 2021; Turner *et al.*, 2017), *publCIF* (Westrip, 2010), *Mercury* (Macrae *et al.*, 2020), *NoSpherA2* (Kleemiss *et al.*, 2021), *GaussView 6.016* (Frisch *et al.*, 2016), *Gaussian 09 Revision A.02* (Frisch *et al.*, 2016), *Molekel 4.3* (Flükiger *et al.*, 2000), *PLATON* (Spek, 2020).

(S)-N-Methyl-1-phenylethan-1-aminium chloride

Crystal data

$C_9H_{14}N^+Cl^-$

$M_r = 171.67$

Orthorhombic, $P2_12_12_1$

$a = 6.7723$ (6) Å

$b = 7.1806$ (5) Å

$c = 20.542$ (2) Å

$V = 998.96$ (16) Å³

$Z = 4$

$F(000) = 368.574$

$D_x = 1.141$ Mg m⁻³

Mo $K\alpha$ radiation, $\lambda = 0.71073$ Å

Cell parameters from 1282 reflections

$\theta = 3.2$ – 30.5°

$\mu = 0.32$ mm⁻¹

$T = 100$ K

Block, colourless

$0.48 \times 0.39 \times 0.37$ mm

Data collection

Bruker D8 Venture
diffractometer

Detector resolution: 10.4167 pixels mm⁻¹

ω and φ scans

Absorption correction: multi-scan
(SADABS; Bruker, 2021)

$T_{\min} = 0.602$, $T_{\max} = 0.650$

45327 measured reflections

4856 independent reflections

4785 reflections with $I \geq 2\sigma(I)$

$R_{\text{int}} = 0.026$

$\theta_{\max} = 36.4^\circ$, $\theta_{\min} = 3.0^\circ$

$h = -11 \rightarrow 11$

$k = -11 \rightarrow 11$

$l = -34 \rightarrow 34$

Refinement

Refinement on F^2

Least-squares matrix: full

$R[F^2 > 2\sigma(F^2)] = 0.011$

$wR(F^2) = 0.024$

$S = 1.14$

4856 reflections

221 parameters

0 restraints

0 constraints

Primary atom site location: iterative

H atoms treated by a mixture of independent
and constrained refinement

$w = 1/[\sigma^2(F_o^2) + (0.0056P)^2 + 0.0168P]$

where $P = (F_o^2 + 2F_c^2)/3$

$(\Delta/\sigma)_{\max} = -0.001$

$\Delta\rho_{\max} = 0.14$ e Å⁻³

$$\Delta\rho_{\min} = -0.22 \text{ e } \text{\AA}^{-3}$$

Absolute structure: Hooft *et al.*, 2010Absolute structure parameter: -0.011 (7)*Special details*

Refinement. Refinement using *NoSpherA2*, an implementation of NOn-SPHERical Atom-form-factors in *Olex2*. 2021 *NoSpherA2* implementation of HAR makes use of tailor-made aspherical atomic form factors calculated on-the-fly from a Hirshfeld-partitioned electron density (ED) - not from spherical-atom form factors. Hydrogen atom H1b was refined isotropically and freely without using calculated ED. Distances and Angles concerning H1b were evaluated by PLATON. The ED is calculated from a gaussian basis set single determinant SCF wavefunction - either Hartree-Fock or DFT using selected functionals - for a fragment of the crystal. This fragment can be embedded in an electrostatic crystal field by employing cluster charges or modelled using implicit solvation models, depending on the software used. The following options were used: SOFTWARE: *Olex2* 1.5 alpha, B1387_0m.wfn as wfn-file, PARTITIONING: *NoSpherA2*, INT ACCURACY: Normal, METHOD: PBE, BASIS SET: def2-SVP, CHARGE: 0, MULTIPLICITY: 1, DATE: 2021.12.08_16:09:30.

Fractional atomic coordinates and isotropic or equivalent isotropic displacement parameters (\AA^2)

	<i>x</i>	<i>y</i>	<i>z</i>	$U_{\text{iso}}^*/U_{\text{eq}}$
Cl1	0.592521 (11)	0.543691 (10)	0.179385 (3)	0.016339 (15)
N1	0.41684 (4)	0.47620 (3)	0.316327 (11)	0.01307 (4)
H1a	0.4079 (9)	0.3344 (8)	0.3230 (3)	0.0295 (14)
H1b	0.4763 (8)	0.4952 (8)	0.2706 (3)	0.0192 (14)*
C1	0.09588 (5)	0.45714 (5)	0.262760 (15)	0.01939 (5)
H1c	0.1708 (9)	0.4643 (10)	0.2151 (3)	0.0406 (16)
H1d	0.0800 (10)	0.3125 (8)	0.2759 (3)	0.0423 (17)
H1e	-0.0497 (8)	0.5137 (10)	0.2588 (3)	0.0407 (17)
C2	0.21347 (4)	0.56000 (4)	0.314781 (13)	0.01314 (4)
H2	0.2339 (7)	0.7048 (6)	0.3009 (2)	0.0231 (12)
C3	0.55360 (4)	0.55695 (5)	0.365038 (15)	0.01794 (5)
H3a	0.5664 (10)	0.7052 (8)	0.3574 (3)	0.0433 (17)
H3b	0.4987 (8)	0.5322 (10)	0.4134 (3)	0.0409 (16)
H3c	0.6979 (9)	0.4918 (9)	0.3592 (3)	0.0420 (18)
C4	0.11585 (4)	0.55281 (5)	0.380803 (13)	0.01459 (4)
C5	0.10068 (6)	0.38632 (5)	0.415554 (17)	0.02390 (6)
H5	0.1630 (10)	0.2592 (8)	0.3963 (3)	0.0438 (17)
C6	0.00496 (6)	0.38292 (6)	0.47550 (2)	0.02996 (8)
H6	-0.0039 (10)	0.2515 (11)	0.5014 (4)	0.062 (2)
C7	-0.07980 (5)	0.54394 (7)	0.500661 (15)	0.02628 (6)
H7	-0.1515 (9)	0.5389 (10)	0.5478 (3)	0.0464 (17)
C8	-0.06743 (5)	0.70924 (5)	0.465812 (16)	0.02150 (6)
H8	-0.1335 (10)	0.8354 (8)	0.4853 (3)	0.0462 (18)
C9	0.03231 (5)	0.71413 (5)	0.406506 (15)	0.01653 (5)
H9	0.0436 (8)	0.8430 (8)	0.3791 (3)	0.0330 (15)

Atomic displacement parameters (\AA^2)

	U^{11}	U^{22}	U^{33}	U^{12}	U^{13}	U^{23}
Cl1	0.02160 (3)	0.01263 (2)	0.01478 (2)	-0.00082 (3)	0.00376 (2)	-0.00023 (2)
N1	0.01278 (8)	0.01374 (9)	0.01268 (8)	-0.00043 (8)	0.00098 (8)	-0.00014 (8)
H1a	0.028 (3)	0.022 (3)	0.038 (4)	-0.001 (3)	-0.002 (3)	0.005 (3)

C1	0.01783 (11)	0.02068 (12)	0.01965 (11)	-0.00110 (14)	-0.00559 (11)	-0.00209 (11)
H1c	0.034 (3)	0.067 (5)	0.021 (3)	-0.008 (4)	-0.006 (3)	-0.008 (3)
H1d	0.051 (4)	0.033 (4)	0.043 (4)	-0.011 (3)	-0.024 (4)	0.002 (3)
H1e	0.020 (3)	0.055 (5)	0.047 (4)	0.007 (3)	-0.014 (3)	-0.004 (3)
C2	0.01310 (9)	0.01303 (10)	0.01329 (10)	-0.00042 (8)	-0.00041 (8)	0.00049 (9)
H2	0.023 (3)	0.016 (3)	0.031 (3)	-0.003 (2)	-0.003 (2)	0.003 (2)
C3	0.01450 (11)	0.01998 (13)	0.01934 (12)	-0.00051 (10)	-0.00309 (9)	-0.00190 (11)
H3a	0.049 (4)	0.016 (3)	0.065 (4)	-0.005 (3)	-0.015 (4)	-0.003 (3)
H3b	0.030 (3)	0.065 (5)	0.028 (3)	-0.009 (4)	-0.001 (3)	0.001 (3)
H3c	0.026 (3)	0.059 (5)	0.041 (4)	0.015 (3)	-0.003 (3)	-0.015 (3)
C4	0.01291 (10)	0.01579 (11)	0.01505 (10)	0.00125 (10)	0.00171 (8)	0.00135 (10)
C5	0.02478 (14)	0.02138 (14)	0.02555 (14)	0.00664 (13)	0.01142 (13)	0.00891 (12)
H5	0.059 (4)	0.028 (3)	0.045 (4)	0.009 (3)	0.020 (3)	0.014 (3)
C6	0.02922 (17)	0.03372 (19)	0.02696 (17)	0.00858 (15)	0.01400 (14)	0.01358 (15)
H6	0.071 (5)	0.050 (4)	0.066 (4)	0.026 (4)	0.034 (4)	0.036 (4)
C7	0.02098 (13)	0.03984 (18)	0.01803 (12)	0.00485 (17)	0.00607 (11)	0.00307 (14)
H7	0.049 (4)	0.062 (4)	0.028 (3)	0.005 (4)	0.020 (3)	0.005 (3)
C8	0.01775 (13)	0.02930 (15)	0.01743 (12)	0.00201 (12)	0.00142 (10)	-0.00627 (12)
H8	0.058 (5)	0.036 (4)	0.045 (4)	0.009 (3)	0.016 (4)	-0.011 (3)
C9	0.01530 (11)	0.01815 (13)	0.01614 (11)	0.00065 (10)	-0.00044 (9)	-0.00345 (10)
H9	0.026 (3)	0.034 (3)	0.039 (3)	0.001 (3)	0.006 (3)	0.003 (3)

Geometric parameters (Å, °)

N1—H1a	1.029 (6)	C3—H3c	1.090 (6)
N1—H1b	1.031 (6)	C4—C5	1.3962 (4)
N1—C2	1.5034 (4)	C4—C9	1.3931 (4)
N1—C3	1.4816 (4)	C5—H5	1.080 (6)
C1—H1c	1.104 (6)	C5—C6	1.3919 (5)
C1—H1d	1.079 (6)	C6—H6	1.085 (7)
C1—H1e	1.070 (5)	C6—C7	1.3905 (6)
C1—C2	1.5237 (4)	C7—H7	1.084 (5)
C2—H2	1.087 (4)	C7—C8	1.3886 (6)
C2—C4	1.5097 (4)	C8—H8	1.087 (6)
C3—H3a	1.080 (6)	C8—C9	1.3935 (5)
C3—H3b	1.075 (5)	C9—H9	1.086 (6)
H1b—N1—H1a	106.0 (5)	H3c—C3—N1	108.5 (3)
C2—N1—H1a	110.2 (3)	H3c—C3—H3a	109.6 (5)
C2—N1—H1b	106.6 (3)	H3c—C3—H3b	109.9 (4)
C3—N1—H1a	109.5 (3)	C5—C4—C2	121.39 (3)
C3—N1—H1b	108.6 (3)	C9—C4—C2	119.33 (3)
C3—N1—C2	115.49 (2)	C9—C4—C5	119.23 (3)
H1d—C1—H1c	108.3 (5)	H5—C5—C4	120.5 (3)
H1e—C1—H1c	109.8 (4)	C6—C5—C4	120.11 (3)
H1e—C1—H1d	107.0 (5)	C6—C5—H5	119.4 (3)
C2—C1—H1c	111.1 (3)	H6—C6—C5	118.4 (4)
C2—C1—H1d	110.0 (3)	C7—C6—C5	120.44 (4)

C2—C1—H1e	110.6 (3)	C7—C6—H6	121.2 (4)
C1—C2—N1	107.44 (2)	H7—C7—C6	119.3 (4)
H2—C2—N1	105.8 (3)	C8—C7—C6	119.62 (3)
H2—C2—C1	110.3 (3)	C8—C7—H7	121.1 (4)
C4—C2—N1	111.62 (2)	H8—C8—C7	119.9 (3)
C4—C2—C1	112.62 (2)	C9—C8—C7	120.10 (3)
C4—C2—H2	108.9 (2)	C9—C8—H8	120.0 (3)
H3a—C3—N1	109.7 (3)	C8—C9—C4	120.48 (3)
H3b—C3—N1	110.1 (3)	H9—C9—C4	118.9 (3)
H3b—C3—H3a	109.0 (5)	H9—C9—C8	120.6 (3)

Hydrogen-bond geometry (Å, °)

<i>D</i> —H \cdots <i>A</i>	<i>D</i> —H	H \cdots <i>A</i>	<i>D</i> \cdots <i>A</i>	<i>D</i> —H \cdots <i>A</i>
N1—H1 <i>a</i> \cdots C11 ⁱ	1.029 (6)	2.088 (6)	3.1075 (3)	170.4 (5)
N1—H1 <i>b</i> \cdots C11	1.031 (6)	2.062 (6)	3.0925 (4)	177.8 (5)

Symmetry code: (i) $-x+1, y-1/2, -z+1/2$.